Analysis of Millimeter Wave FMCW Radar System for Ranging and Sensing Applications

A Major Qualifying Project

Submitted to the Faculty of

Worcester Polytechnic Institute

In partial fulfillment of the requirements for the

Degree in Bachelor of Science

in

Physics

By

_____

Jacob Bouchard

Date: 4/25/2019

Project Advisor

_____

Professor Douglas Petkie

Abstract

For almost a century, work has been proceeding to continuously improve radio detection and ranging (radar) systems. The development of frequency-modulated continuous-wave radar (FMCW) systems and the application of millimeter waves, have allowed radar systems to measure vital signs. No experimental work has been performed to test whether FMCW radar systems are able to measure displacements on the order of vital signs when multiple moving targets are in the path of the beam. This paper presents the construction and analysis of an FMCW radar system operating at a central frequency of 96 GHz being linearly modulated at 10 kHz over a bandwidth of amplitude 96 MHz, culminating in the measurement of two targets moving with displacements similar to vital sign signatures (~300 μm).

Acknowledgements

I would like to thank my family for their continued support.

I would like to thank Jim Eakin for his invaluable help in the lab

Most importantly I would like to thank my advisor Professor Doug Petkie for his help and insight and for countless hours spent in and out of the lab working with me.

Table of Contents

1. Introduction

Since its inception almost a century ago, radio detection and ranging (radar) systems have been put to use in a variety of important applications [1] from early warning missile detection systems, and missile guidance systems, to weather detection radars, airport traffic monitoring and even automatic door openers. Advancements in solid-state technology have given rise to continuous-wave (CW) frequency-modulated continuous-wave (FMCW) radar that are being used in automotive applications such as automatic follow distance systems and back-up obstacle detection. FMCW radar systems send out a continuous wave whose frequency is swept according to a specific waveform. The reflected signal from the target has embedded information in the phase and intensity that can be used to determine target's range, displacement, velocity, and acceleration. Work has been done to test the feasibility of these systems for the monitoring of single targets [2] for vital sign signatures at standoff distances (~1-5 m) [3]. Multiple targets complicate the measurements since the reflected beam contains information about all targets in the path of the beam. We were interested to see if by using a lock-in detection technique to measure the harmonics of the modulating beam, we would be able to separate the signals from each target for the simultaneous monitoring of displacement of several objects.

The use of frequencies between 30 GHz and 300 GHz (the millimeter wave (mmW) band) in an FMCW radar system have four distinct advantages:

1. The small wavelengths in this band (1 mm-10 mm) should allow very small movements (~10-100 μm) to be resolved and monitored.

2. The shorter wavelengths mean that higher spatial resolution can be realized with relatively small optical apertures. This can allow for individual targets to be isolated, or an imaging system to be developed.

3. Transmission through common dielectrics, such as clothing, with sufficient atmospheric propagation for effective use at distances on the order of ~100 m.

4. With the introduction of 5G and 6G wireless and communication bands on the horizon, radar transceivers in the millimeter wave band will become more available, and perhaps be ubiquitous and open up the possibly of a multitude of secondary applications.

These advantages can allow a mmW radar system to identify individual targets in a cluttered environment where multiple targets exist. For environments where non-contact vital sign sensing, such as home health care or military target evaluation, is of interest these advantages can also be leveraged. The primary purpose of this project is to longitudinally resolve two moving targets within the same beam or resolution element, which has not been possible using continuous-wave systems while maintaining the capability to monitor vital signs or other small displacements or micro-Doppler signatures.

1.1 Goal

The goal of this project is to characterize a mmW FMCW radar system and provide a proof-of-principle to simultaneously resolve and monitor the displacement of two separate targets. The project can be broken into two primary objectives:

1. Assemble an FMCW radar and use single moving targets to characterize the system

First, an FMCW radar system was built and studied in order to understand its operation and performance. Measurements were taken of a single moving target across a measurement area of approximately 3 m. In order to record and process this data custom LabVIEW data acquisition and IgorPro data analysis programs were designed to characterize the systems performance that included the incorporation of lock-in detection technique that are key to resolving multiple targets.

2. Measure two moving targets at two distinct ranges

Once we accurately measured the movement of a single target, we studied how well the system could measure two distinct moving targets. These two targets would be moving with displacements on the order of vital signs (~100 μm and frequencies ~1 Hz). This would provide a proof-of-principle and serve as a foundation to further test the limits of simultaneously monitoring the displacement of multiple targets over large distances using this technique.

2. Background

2.1 Radar Systems

Radio detection and ranging (Radar) systems have been used in a wide variety of applications for almost a century [1]. At their core, these systems are simply a way to gain information about a target through its interaction with electromagnetic waves, including its speed, distance from the antenna, and its identification. There are three primary types of radar systems and a brief description of each system follows.

2.1.1 Pulsed Radar

Pulsed radar systems were the earliest type of radar systems that were put into practical use during World War II [4] and are still in use today as weather radars and long range early warning systems. Pulsed radar systems work by sending out a relatively powerful and short signal at a target. The system then goes into receiving mode to listen for the pulse that was reflected off of the target. By measuring the round trip time of flight of the pulse, also called the running time, the line of sight distance from the radar to the target can be determined by the equation, $\Delta x = \frac{c*t}{2}$ where c is the speed of light and t is the running time [5]. The primary limitation of pulsed radar systems is that they cannot resolve small displacements due to finite pulse widths and durations (i.e. ~millimeter displacements correspond to a 6 picosecond change in the time of flight). This makes them unsuitable for applications such as vital sign sensing.

2.1.2 Continuous-Wave Radar

Continuous wave radar systems utilize a beam consisting of a single, pure carrier frequency. When this beam hits a target, some of it is reflected back toward the system. This

reflected beam has a phase that is different than the emitted beam. This phase change can be used to monitor the displacement of the target according to the equation $\Delta\varphi = 2\pi \left(\frac{2\,(\Delta r)}{\lambda} \right)$ where Δr is the displacement of the target along the beam path and λ is the wavelength of the emitted beam. This method, or interferometry, allows for the measurement of relatively small displacements (<100 µm) [6]. Continuous wave radar systems are well suited to applications where you are only interested in looking at one target. These systems fail when more than one target is in the emitted beam path. This is due to the fact that if two targets are in the beam path, the reflected beams from both targets will mix when coming back to the antenna. Extraction, or deconvolution from a complex superposition of target signatures, of each target can be extremely difficult and limit the use of a continuous wave radar system in a complex or cluttered environment.

2.1.3 Frequency-Modulated Continuous-Wave Radar

Frequency-modulated continuous-wave (FMCW) radar systems emit a beam whose frequency is (typically linearly) modulated over a determined bandwidth. This frequency modulation gives rise to what are known as range bins. Range bins exist along the path of the radar beam and have a length (δ) determined by the modulation bandwidth (B) [7], $\delta = \frac{c}{2B}$. These range bins correspond to harmonics of the modulation signal. This allows us to "tune" into harmonics and measure a target in a particular range bin. Due to its similarity to a continuous wave system, we can also use the phase changes of the reflected wave to track the displacement of a target within a particular range bin.

2.2 Millimeter-Waves for Radar Sensing

Millimeter-waves are electromagnetic waves that have a very high frequency which is defined as being between 30 GHz and 300 GHz. The short wavelengths of the band (10-1 mm) allow for small changes in displacement to be monitored (i.e. $\frac{1}{100} \lambda \approx 10 \ \mu m$). Millimeter-waves are commonly used in concealed weapons detection as they can easily pass through common clothing barriers [8]. These two characteristics of millimeter-waves are particularly attractive for radar applications as it would allow a system to accurately monitor vital signs by monitoring displacements of the surface of the skin through clothing [9] and are currently a technology deployed in airports for personnel screening [10]. A large amount of work has also been done to develop millimeter wave imaging systems [11].

With the 5G and 6G wireless communication revolutions on the horizon, millimeter-wave sources will be omnipresent in our lives. Telecom giant Verizon began rolling out its 5G service in the United States, which operates in the 28 GHz range, in 2019 with the first service being switched on in early April [12]. Researchers in the communication field are predicting that 6G standardization is not too far off either [13]. These developments in millimeter-wave based communication has two provides other systems based on millimeter waves two important advantages. Sources of millimeter-wave radiation will become significantly cheaper, and systems such as vital sign monitors can easily be integrated into communication networks and into the Internet of Things (IoT) for sensing applications.

2.3 The Michelson Interferometer

The Michelson interferometer was invented by Albert Michelson for use in the famous Michelson and Morley experiment in 1887 [14]. The interferometer, whose geometry can be seen in Figure 1, compares the phase of the radiation reflected from the two mirrors where the phase depends on the path differences.
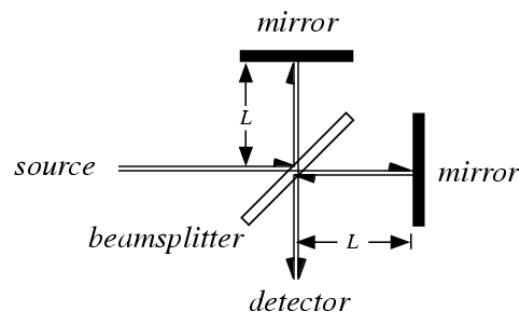
Figure 1: The geometry of a simple Michelson interferometer showing the source, 50/50 beam splitter, two mirrors, and the detector [15].

The Michelson interferometer works by emitting electromagnetic radiation from a source, splitting the radiation equally using a 50/50 beam splitter, reflecting the radiation off of two mirrors, and recombining the two beams at the detector. For the purposes of this paper, the intensity of radiation at the detector, as a function of the intensity of the emitted radiation I_0, the wavelength of the emitted radiation λ, and the optical path difference between the two arms $2x$, where x is the physical path difference in the two arms, can be approximated as

$I \sim I_0 \cos\left(2\pi\left(\frac{2x}{\lambda}\right)\right)$. We can see that for the case where the emitted beam is of a single wavelength λ, the intensity goes to zero when the optical path difference is some integer of $\lambda/2$. When used in an FMCW radar system, where the source's wavelength is varied over a certain bandwidth, the equation for the Michelson interferometer can be written as

$I \sim I_0 \cos\left(2\pi\left(\frac{B}{c/2x}\right)\right)$ where the substitutions $f = \frac{c}{\lambda}$ and $f = B$ where B is the bandwidth of

the linear sweep in the frequency, have been made. When $\left(\frac{B}{c/2x}\right)$ is an integer n(i.e. within a

range bin), the intensity signal is a cosine wave with n complete periods as the target is in the

center of a range bin. The number of cycles for a given distance then allows the range of the

target to be identified as in one of the range bins.

2.4 Lock-In Amplifiers

A lock-in amplifier is a tool that is used to detect small AC signals by using phase-

sensitive detection to differentiate the signal from noise or to isolate a particular harmonic of the

modulation frequency (harmonic detection) to improve the signal-to-noise ratio [16]. Phase

sensitive detection works by combining, or multiplying, the input signal with a reference signal,

or a multiple of the reference frequency to identify a harmonic of the fundamental modulation.

Each multiple of the reference frequency corresponds to a target in a particular range bin based

on the ratio $\left(\frac{B}{c/2x}\right)$. There are a few different ways to process a signal with a lock-in amplifier but

for the purposes of this project we are only interested in in-phase (I) and quadrature (Q) signals.

I-signals are simply the input signal combined with the reference wave, the Q-signal is the input

signal combined with the reference signal whose phase has been shifted by 90˚. By utilizing I

and Q measurements we were able to process our data more easily as our data analysis routines,

that were developed for a previous continuous wave radar system, were made to process I and Q

signals. These routines would take the raw I and Q signals, box smooth them to eliminate noise

and find the phase. Here the phase is defined as $\varphi(t) = \left[\tan^{-1}\left(\frac{V_Q(t)}{V_I(t)}\right)\right]$, this phase was

discontinuous. To get displacement data from this discontinuous phase, a phase unwrapping

algorithm was applied where $\varphi(t) = 2\,\pi\left(\frac{2\,x(t)}{\lambda}\right)$ and the displacement was scaled according to

$x(t) = \frac{\lambda}{2}\frac{\varphi(t)}{2\,\pi}$.

3. Methodology

The goal of this project was to construct and characterize an FMCW radar system based on the Michelson interferometer and simultaneously measure two distinct moving targets with displacements similar to vital signs (~10-100 μm). To realize our goal, we formalized the following research objectives:

1. Construct the FMCW radar system.

    a. Assemble and align the optical components of the system.

    b. Optimize the conditioning electronics (amplifiers and filters) to match the digitization of the DAQ

    c. Develop and modify existing data collection and data analysis routines.

2. Characterize the behavior of the system with a single, idealized target.

    a. Take measurements of large displacements (~20 mm > λ) to test the system and our data analysis routines.

    b. Take measurements of small displacements (~2 mm ≈ λ) to test the resolution of the system.

    c. Take measurements of displacements on similar order of magnitude of vital signs (~100 μm < λ).

    d. Characterize the behavior of the intensity of different harmonics at the detector over a large range.

3. Characterize the behavior of the system with two moving targets.

    a. Measure two moving targets in different range bins, with similar but distinct motions, positioned in the beam.

    b. Determine if the signatures of the targets interfere in different range bin interfere

       with each individual signature.

3.1 Objective 1: Construct the FMCW Radar System

A basic layout of the system is present in Figure 2 with the components listed in

Appendix A.
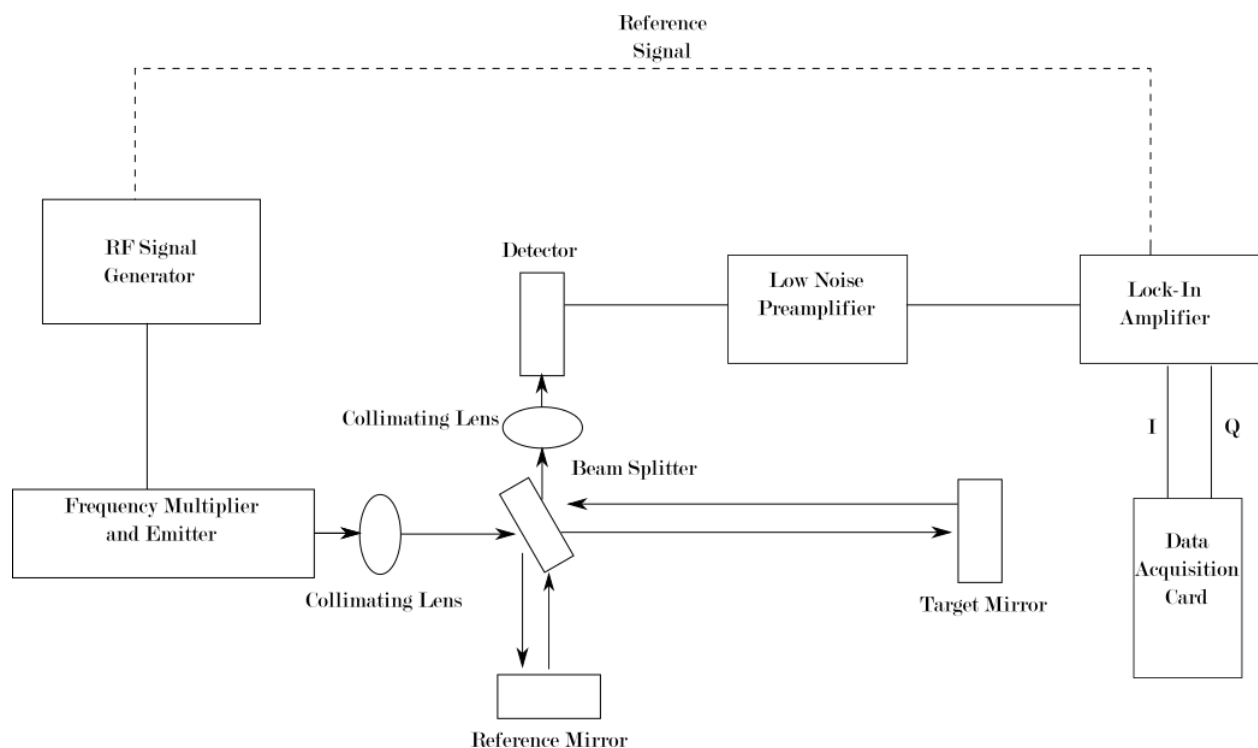
Figure 2: A simplified layout of the FMCW radar system developed for this project.

For the purposes of this project, the RF signal generator was set at 8 GHz, this signal was

passed through a combined frequency multiplier and emitter, the multiplier upped the signal to

96 GHz ($\times$12) through an active $\times$4 multiplier and a passive $\times$3 multiplier with an output power

on the order of 1 mW. The signal was swept as a linear ramp function at 10 kHz over a

bandwidth of amplitude 192 MHz (peak-to-peak deviation), the frequency of the ramp function

as was a reference signal for the lock-in amplifier. The detector was a single signal detector; the signal was passed through a low noise preamplifier set as a bandpass filter between 10 kHz to 1 MHz with a gain of 100. The signal from the preamp was passed to a lock-in amplifier set to take I and Q measurements, the harmonic of the lock-in amplifier was set to the range bin we were interested in. From the lock-in, the I and Q signals were passed to a data acquisition card, the digitization rate of the card was set between 1000-10000 Hz depending on the velocity of the displacement being measured.

3.1.1 Component A: Assemble and Align Components of the System

In order to safely assemble these components, some of which are very sensitive to electro-static discharge, care was taken to avoid ESD events and monitor input powers into the frequency multiplier chain. The components were laid out on an optical table and were roughly aligned by sight. Two ~6 cm Teflon lenses with ~200 mm focal lengths were used to collimate the mmWs from the horn (~50 mm aperture) of the source and to match the received mmWs onto the horn of the detector. A ~15 cm Mylar beam splitter optimized for 50/50 spitting was used to couple to the reference ~60 mm diameter corner cube reflectors and the target arm. In order to refine the alignment, various components were moved very slightly in the x, y, and z directions by hand until the signal at the detector was maximized.

3.1.2 Component B: Modify Existing Data Collection and Data Analysis Routines

As mentioned before, this system was constructed from a previously existing continuous wave radar system [9] so much of the data collection and data analysis routines could be used and/or modified for this application. The data collection routine from the previous system, was a LabVIEW VI that translates the linear stage a certain displacement at a specified velocity.

Another VI was created based off of the original VI that allowed us to collect data without having to translate the linear stage, but instead collected data over a specified time.

The data analysis routine from the previous system was an IgorPRO module that performed the phase unwrapping algorithm and scaled the displacement. For the purposes of our investigation, the module was modified to allow us to choose whether or not we removed the DC offset from our data, and over how many points we smoothed our raw data. This module allowed us to perform all of these tasks automatically and quickly.

3.2 Objective 2: Characterize the Behavior of the System with a Single, Idealized Target

Before attempting to measure two moving targets, we wanted to confirm that our system was able to accurately measure the displacement of a single target.

3.2.1 Component A: Take Measurements of Large Displacements (~20 mm) to Test the System and Our Data Analysis Routines

In order to test our system and data analysis routines, we wanted to attempt to measure large displacements (~20 mm) compared to the wavelength of 3.125 mm. To do this we attached a 6 cm diameter, corner cube retroreflector that would reflect the radiation in back at the incident angle, to a linear stage and centered it in the beam. Using our custom VI, the stage was translated 20 mm (or larger distances). The data from this test was put through our IgorPro routine. Our initial results had a very poor signal to noise ratio that made it impossible to differentiate the position to get velocity. The source of this noise was determined to be the Stanford Research SR830 lock-in amplifier which introduced a large amount of oscillatory digital noise. Once the

amplifier was replaced with the Anfatec USB lockin 250 lock-in amplifier, we confirmed that our system was indeed working and could measure large displacements. These measurements were taken in the three range bins that fit on our optical table.

3.2.2 Component B: Take Measurements of Small Displacements (~2 mm) to Test the Resolution of the System

Once we had confirmed that our system could accurately measure large displacements, we wanted to confirm that our system had great enough resolution to measure small displacements (~2 mm) that were on the order of magnitude of the wavelength. To do this, we followed the same procedure as above but instead of translating the stage 20 mm, we translated it 2 mm. This test was also successful and it should be noted that the number of interference fringes (or periods) was approximately one period. At this point, the DC offset due to bias voltages can cause the phase unwrapping algorithms to fail as they assume a zero DC offset.

3.2.3 Component C: Take Measurements of Displacements on Similar Order of Magnitude of Vital Signs (~100 μm)

Once we were confident that our system could measure displacements on the order of several millimeters, we wanted to verify that we could measure displacements on the order of vital signs which are approximately 100 μm. To do this we covered the cone of a 8 cm inch speaker with tinfoil and drove it with a Pasco signal generator at 1 Hz. This speaker was placed in the path of the beam and the displacement was measured. We lowered the amplitude of the speaker's oscillation to the lowest magnitude that the signal generator would allow. This test confirmed that our system could measure displacement on the order of vital signs for subwavelength displacements. While this was not successful on all trial runs, it was successful

on a majority of tests. While successful, we feel that further studies are needed and a calibration procedure may be needed that involves displacement over several wavelengths to ensure the phase unwrapping algorithm is successful.

3.2.4 Component D: Characterize the Behavior of the Intensity of Different Harmonics at the Detector Over a Large Range

Before introducing a second reflector into the beam path, we wanted to study how the intensities of the harmonics varied across the three range bins that fit on our optical table. To do this a corner cube retroreflector was placed in the beam in slid backward along the length of our optical table. This test was performed for harmonics 1-5 through range bins 1-3 over a distance of 2.6 m. Results are shown in section 4.1.4.

3.3 Characterize the Behavior of the System with Two Moving Targets

The key experiment for this project was to determine whether or not it would be possible to simultaneously measure two moving targets within the beam located in different range bins.

3.3.1 Measure Two Moving Targets in Different Range Bins Positioned in the Beam

In order to carry out this experiment, two tinfoil covered speakers driven by two separate function generators were placed in two separate range bins. In order to not completely block out the beam, the smaller (~5 cm diameter) of the two speakers was placed in range bin two oscillating at 0.706 Hz. A larger speaker, oscillating at 1.00 Hz was placed on a separate optical breadboard off of the edge of the optical table that was positioned in range bin four. With both

speakers oscillating measurements were taken with the lock-in set to harmonic 2 and harmonic 4.

Results are shown in section 4.2.2.

4. Findings and Analysis

This chapter contains the results from our experiments as well as our analysis of these results. When multiple targets were placed in the beam, we discovered that our system could detect and resolve multiple moving targets in different range bins. The chapter has been split into two parts, the single target and multiple target experiments, to differentiate between the tests being performed.

4.1 Single Target Experiments

This section includes the results from our experiments that involved a single target. These experiments include large and small displacement tests, as well as an analysis of the interaction between harmonics 2 and 3.

4.1.1 Large Displacement Tracking

The large displacement experiments were done to confirm that our system was able to track displacements and that our data analysis routines were working as expected. For this test, the linear stage was placed in the second range bin and translated backwards 20 mm at 10 mm/s. The raw I and Q data can be seen in Figure 3. We were primarily concerned with the phase of our raw signal φ which is defined as $\varphi = \tan^{-1}\left(\frac{V_Q}{V_I}\right)$. The phase of this signal is seen in Figure 4. This phase is discontinuous and, in order to extract relevant displacement information from the phase, a phase unwrapping algorithm built into IgorPro was applied to the data to make the phase a continuous function. The displacement measurement from this experiment can be seen in Figure 5. Ignoring the acceleration present when the stage begins moving, we assume that the movement of the stage, and therefore the target, is linear and at a constant velocity. The results of

a linear fit performed on the displacement, between 0.2 and 1.8 seconds, can be seen in Figure 6. The residual reveal an approximately 40 mm deviation from a linear translation, which fall outside of the specification of the accuracy of the linear stages. However, given all of the testing, we feel confident that is accurately reproducing the motion of the target. An interesting observation of the data from tests not presented here involved monitoring the motion of the retroreflector when the stage stops moving. The retroreflector has a significant mass and we mounted ~20 cm above the linear stage with standard optical components (optical posts and post holders). This creates the opportunity for the retroreflector to undergo damped oscillation (i.e. ring down) whenever the stage came to an abrupt stop. The initial amplitude of these oscillations (when the mirror was stopped) was on the order of 500 μm with a ring down time of 10 seconds. We feel the deviation, or residuals to the linear fit, are showing the retroreflector 'oscillating' at the end of the ~20 cm post that it is mounted to. In this case, we are actually monitoring the vibrational dynamics of the optical system that we constructed to test the system. We found no further explanations for this deviation and plan to reduce the moment arm (height of the optical post) in future experiments to confirm this assumption
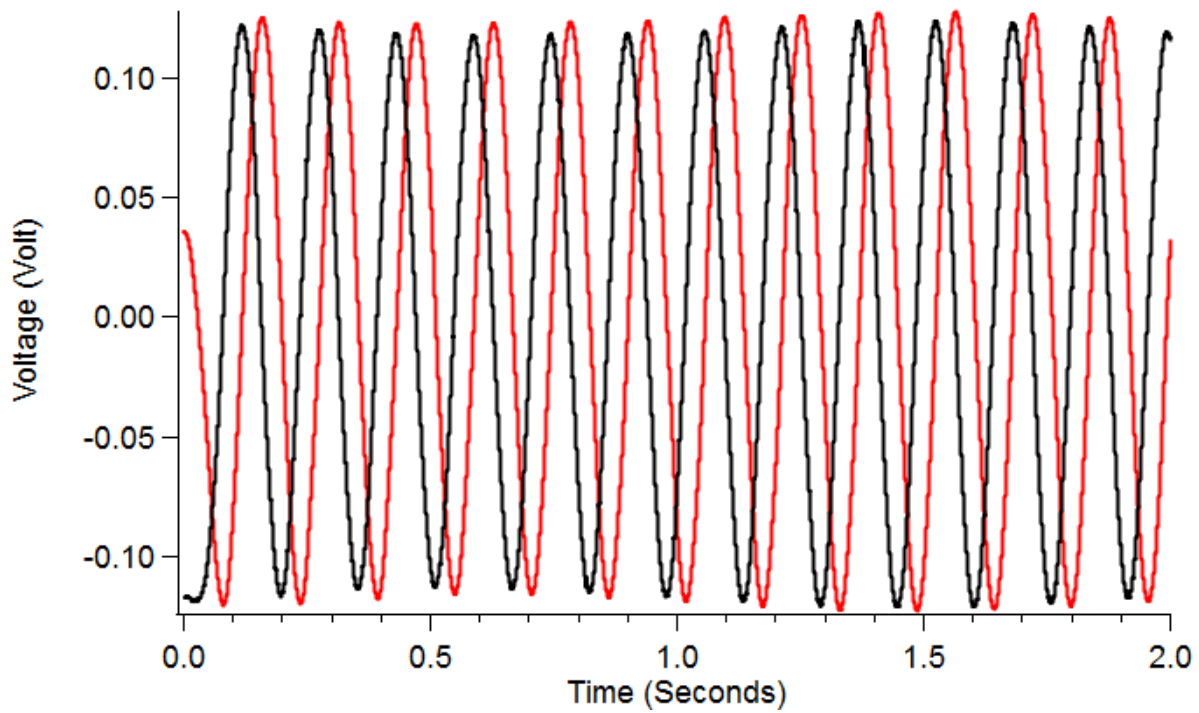
Figure 3: The raw I and Q data from the large displacement, single target, test. Note that I (the red wave) and Q (the black wave) are out of phase by 90˚
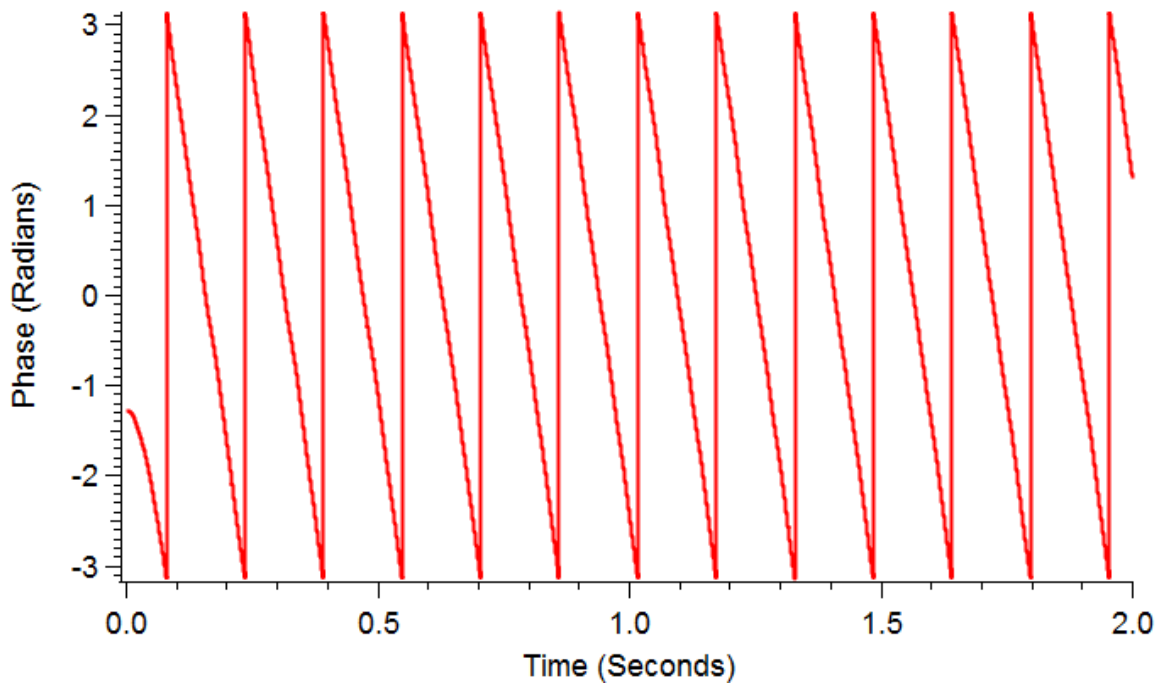
Figure 4: The phase of the signal from the large displacement experiment. Note the discontinuous nature of the phase that ranges from -2π to 2π.
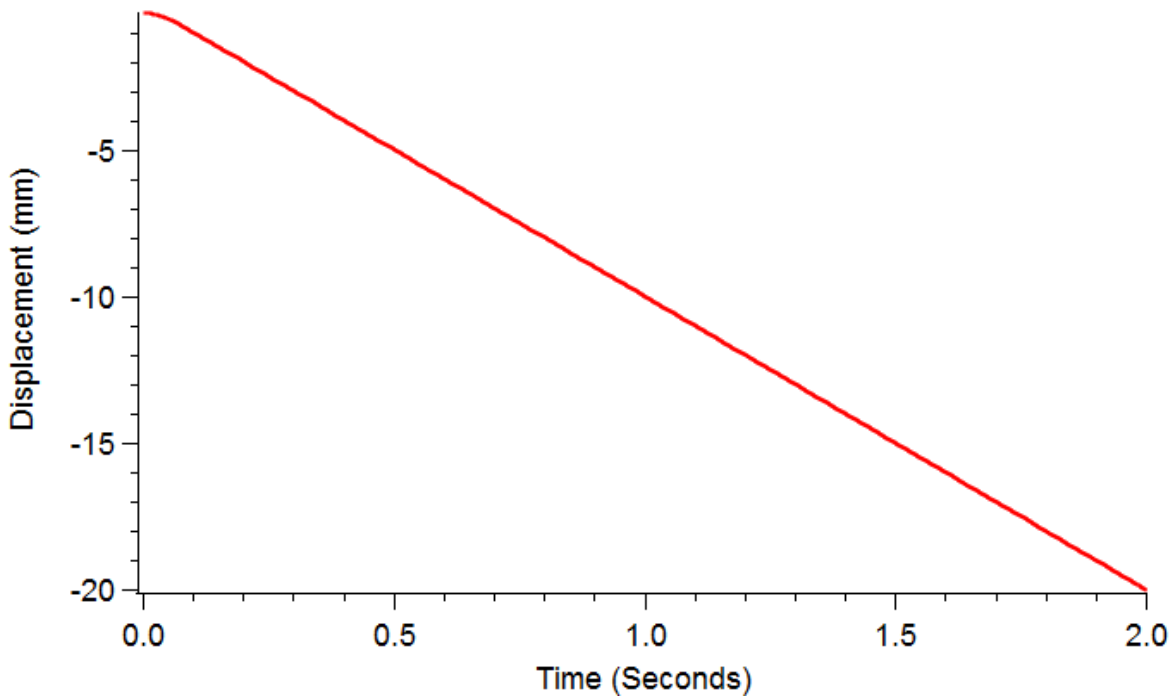
Figure 5: The displacement information from the large displacement experiment. Note the acceleration curve present between 0 and 0.1 seconds.
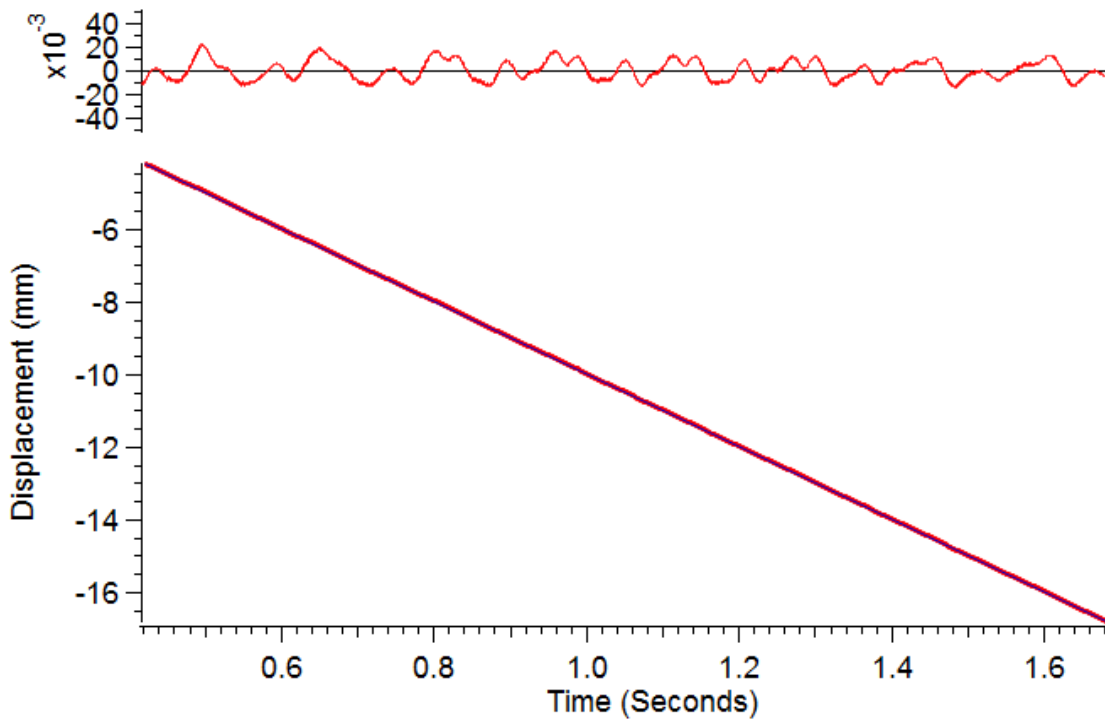
Figure 6: The linear fit of the displacement from the large displacement experiment. The residuals are at the top of the graph. Note that the residuals are on the order of ~20 μm, these could be due to the movement of the stage.

These tests were performed across the length of our optical breadboard (~2.5 m), to confirm that the results were consistent over a large range. The results of this experiment confirmed that our system was able to detect and measure displacements and that our data analysis routine was able correctly interpret the data.

4.1.2 Small Displacement Tracking

Once we had established that our system and data analysis routines could accurately track and interpret large displacements, we took measurements of small displacement (~2 mm and on the order of the wavelength) at 1 mm/s. This was to confirm that our system could track displacements that were smaller than before but still easy to observe. These tests were performed in the three range bins that fit onto our breadboard. The displacements result from range bin 2 is presented in Figure 7.
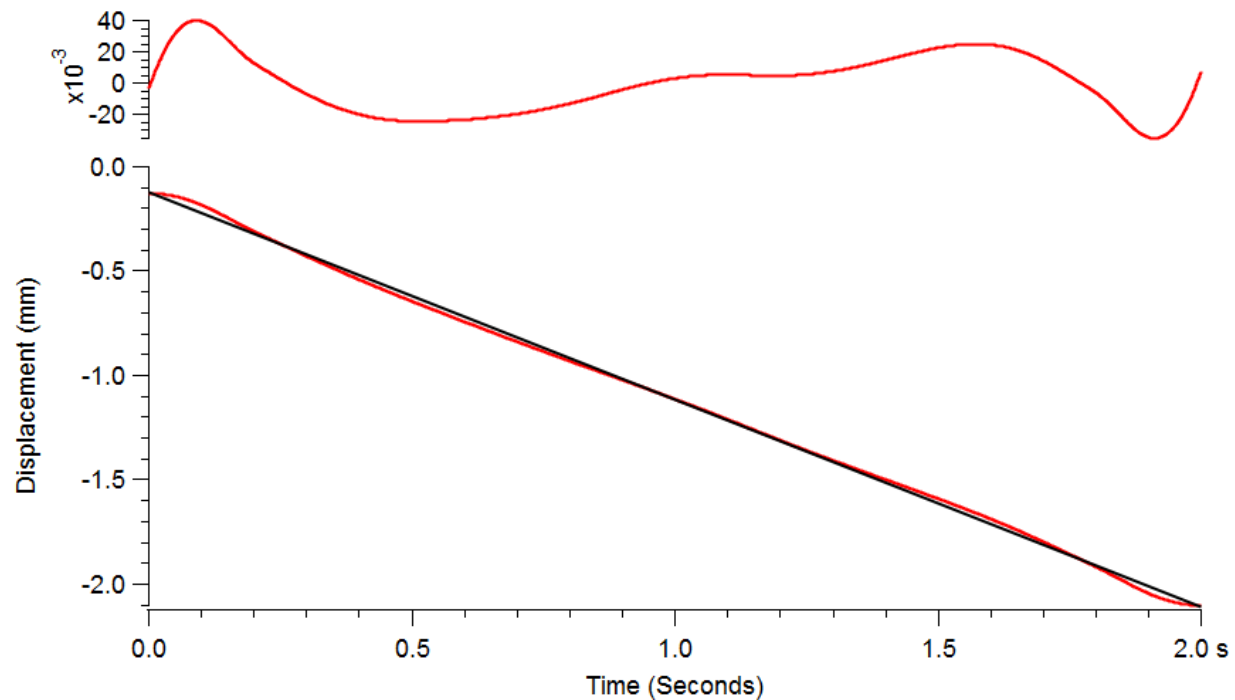
Figure 7: The displacement result from translating the linear stage -2 mm at 1 mm/s. Notice the more pronounced acceleration profiles.

The results from this experiment proved to us that our system and data analysis routines could track and interpret small displacements (~2 mm). The residuals of a linear fit (seen at the top of the graph) demonstrates that there were deviations of approximately 40 μm. These deviations may have been due to a combination of the small translation distance and the acceleration profile of the linear stage.

4.1.3 Displacements on Similar Order of Magnitude of Vital Signs

Our primary interest for applications of this system is for vital sign monitoring from multiple targets. Before attempting to measure multiple targets, we wanted to confirm that our system could measure displacements on the same order of magnitude as vital signs which include the sub-wavelength region of < 1 mm. To do this we placed a tinfoil covered speaker driven at 0.706 Hz was placed in the second range bin and its motion was measured for 10 seconds. This displacement measurement can be seen in Figure 8.
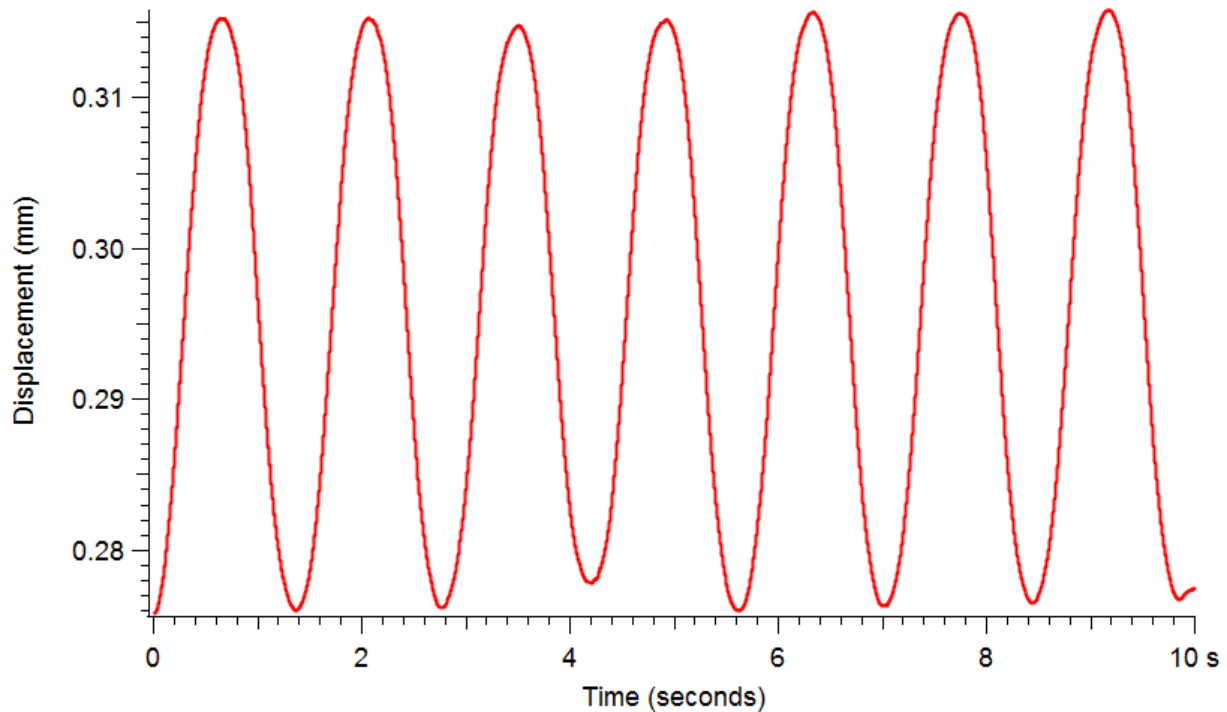
Figure 8: The displacement of a tinfoil covered speaker oscillating at 0.706Hz. Note that the absolute displacement is 40 μm.

This test confirmed that our system was capable of measuring displacements on the order of vital signs. Performing a curve fit we found that the frequency was accurately measured as 0.715 Hz and the amplitude was constant.

4.1.4 Tracking the Behavior of Harmonics Across Range Bins

In order to understand how the intensities of different harmonics behave over different range bins, we measured harmonics 2 and 3 across range bins 1, 2, and 3. A graph of the intensity of the harmonics versus distance can be seen in Figure 9.
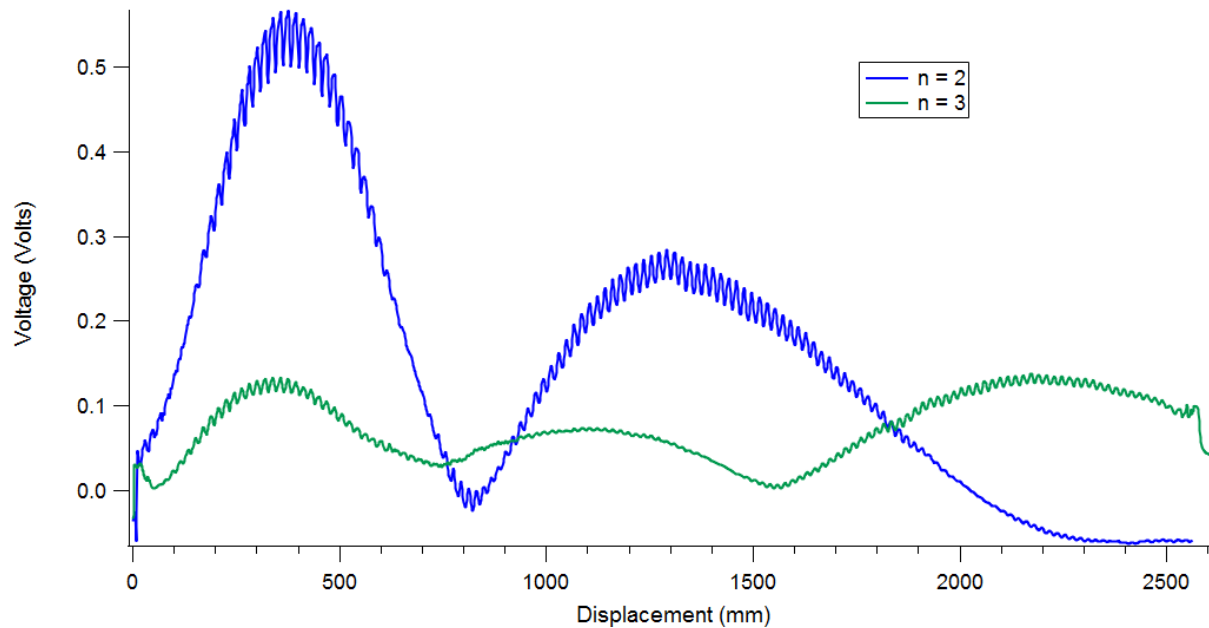
Figure 9: A graph of the intensities of harmonic 2 and 3 versus distance. The range bins here have width 750 mm.

We see that both harmonics 2 and 3 have large peaks in the first range bin ~78 cm and, this is likely caused by strong internal reflections that exist within that range bin between the optical elements within the system. These reflections quickly die off as the target moves out of that bin. At the distance 1300 mm, which is in the second range bin, the second harmonic has a peak in intensity. This peak begins to die at 1500 mm which corresponds to the limit of the second bin. Harmonic 3 has its peak at around 2100 mm which is within the third bin and begins to die out at 2250 mm. A key takeaway from this experiment is that the peaks don't die out immediately at the limit of the bin, they die out more gradually. This gradual die off and ramp up of the intensities and coupling between range bins may contribute to cross talk between targets in separate bins and contribute to uncertainties in simultaneous displacement sensing.

4.2 Multiple Target Experiments

Once we understood the performance of our system measuring single targets. We were ready to measure two targets positioned in the beam.

4.2.1 Single Target Moving

To ensure that having two targets in the beam did not hinder our systems ability to measure a single moving target, we placed one target in the second range bin and kept it stationary. We placed another target on a separate optical breadboard off of the optical table located in the fourth range bin and had it oscillate at 1 Hz. The measurement taken of the fourth harmonic is in Figure 10.
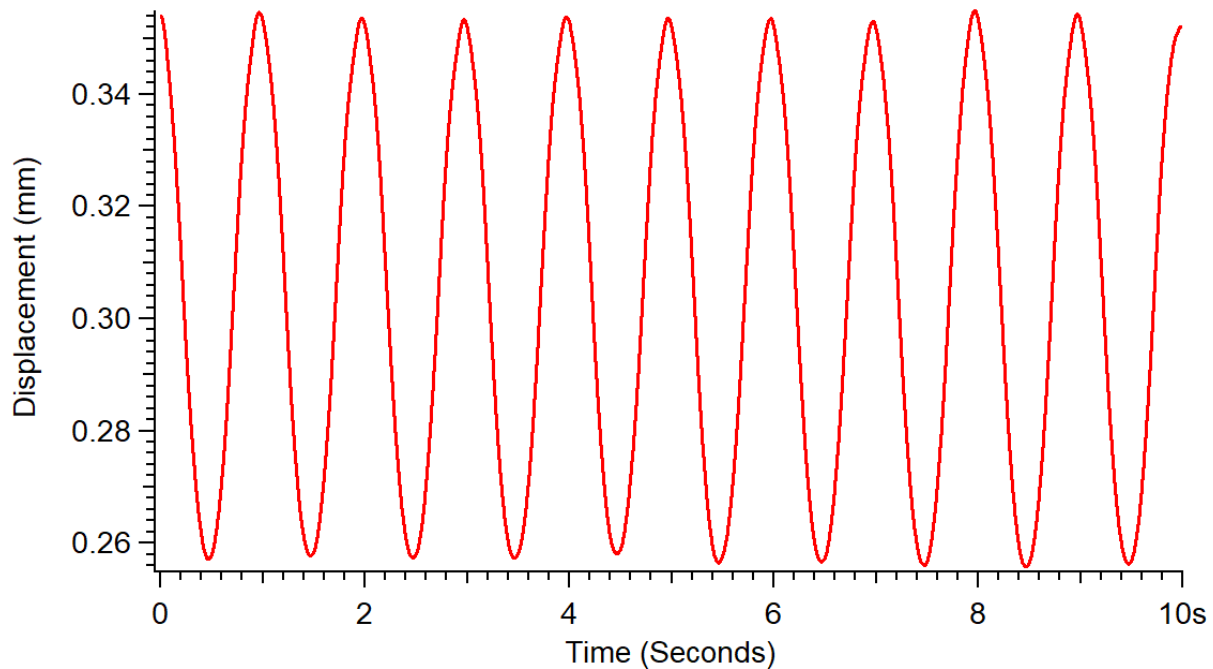
Figure 10: Displacement measurement taken in the fourth harmonic of a target in the fourth range bin oscillating at 1 Hz. This measurement was taken when there was a stationary target in the second range bin.

We found that the amplitude of the oscillation was 90 μm. This measurement confirmed that stationary targets in lower range bins do not affect measurements in higher range bins. This

result was very encouraging and allowed us to move onto measurements of multiple moving targets in different range bins.

4.2.2 Two Moving Targets

Our key experiment in this project was to test if our system could adequately measure two moving targets in two different range bins. To do this, the target in the second range bin was set oscillating at 0.706 Hz and the target in the fourth range bin was set oscillating at 1.0 Hz. Measurements were taken of the second and fourth harmonics to determine the effectiveness of our system. Measurements from this experiment are seen in Figures 11 and 12.

The measurement of the second harmonic displayed a normal displacement pattern of a target oscillating at 0.706 Hz. The fourth harmonic shows a displacement pattern of a target oscillating at 1 Hz, however there is an unexpected modulation of the intensities in bin 4. This modulation can be seen when comparing the amplitudes of the displacement from this test with the amplitudes of the displacement in the previous experiment. We expect the amplitudes to be the same. Since this modulation is not present when the target in the second range bin was stationary, we can say that it is caused by some interaction between the displacement signals from bin 2 and 4. We did not observe any significant impact on the measurement in bin 2.
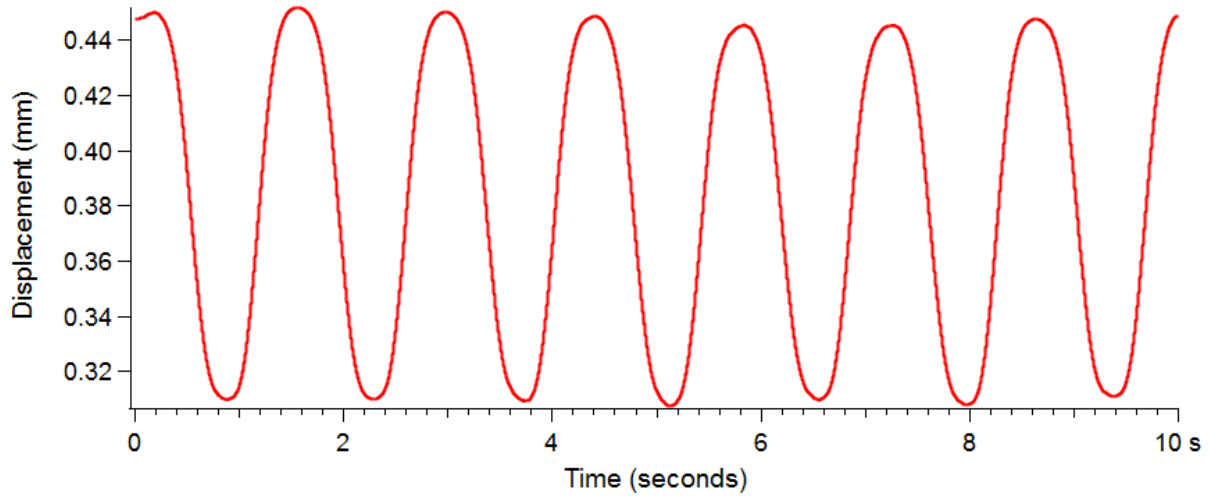
Figure 11: Measurement of the second harmonic where there was a target in the second range bin was oscillating at 0.706 Hz and a target in the fourth range bin was oscillating at 1 Hz.
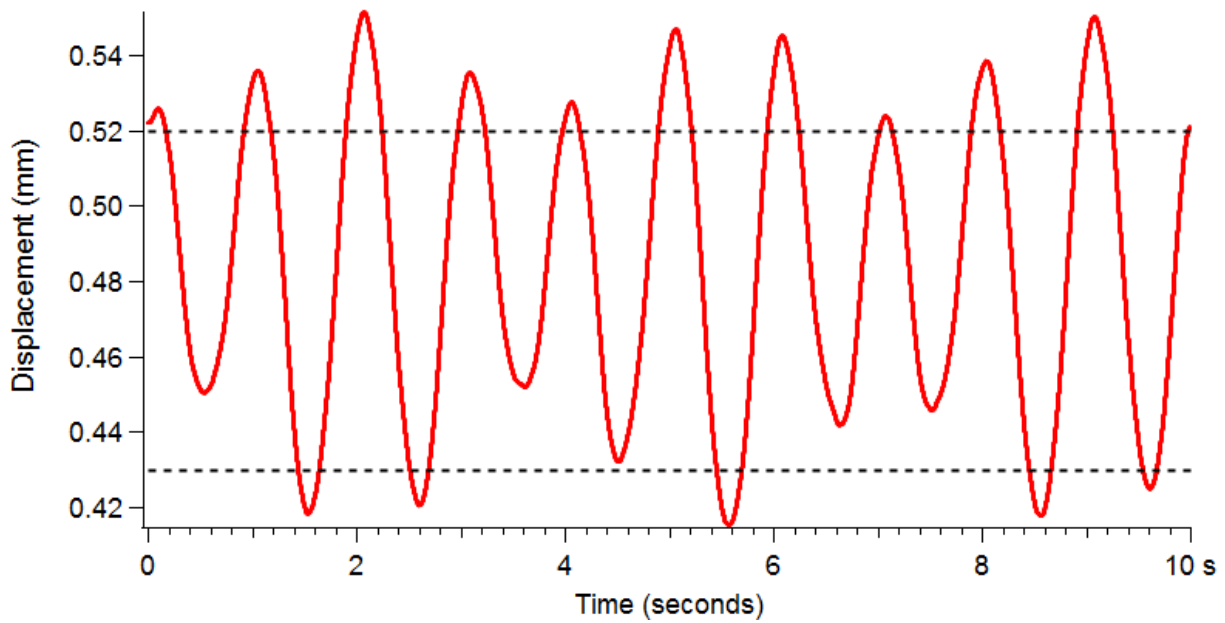
Figure 12: Measurement of the fourth harmonic where there was a target in the second range bin was oscillating at 0.706 Hz and a target in the fourth range bin was oscillating at 1 Hz. The dashed lines represent the amplitude of the displacements from Figure 10.

5 Conclusions and Further Work

The objective of this project was to determine whether or not a millimeter wave FMCW radar system operating at a central frequency of 96 GHz being modulated a frequency of 10 kHz over a bandwidth of amplitude 96 MHz was capable of measuring the displacements of multiple targets at different ranges that were on the order of vital signs. Measurements of this type had never been performed before, to our knowledge, and the applications of such a system are very exciting.

5.1 Conclusions

We found that our system was able to measure the displacement of multiple targets that were on the order of vital signs. We discovered that displacements in lower bins has some effect on the measurements of displacements in higher bins, but not the reverse. This effect is most likely due to the slow die off of the intensity of harmonics in higher range bins. We were able to accurately measure the frequency of oscillation for two targets in different range bins. For the target that was further away, we observed a sort of 'beat note' phenomena and the amplitude of the oscillation (90 μm) oscillated about this value with deviations up to 30 μm. The oscillation of this distant target had no effect on the measurements of the oscillations of the closest target.

5.2 Recommendations for Future Work

Further work must be done to investigate the interactions between displacements in different range bins. A problem that we had when trying to study this phenomenon is that we did not have access to oscillating targets with a consistent radar cross section. The targets that we

were using were curved speakers with tinfoil taped onto the cone. This the inconsistent nature in the surface of these targets made it hard to determine what part of the phenomena that we were observing came from range bin cross talk or the deformation of our targets surface.

In order to push our system to its fundamental limit of the smallest displacement that it can measure, we would like reduce all unwanted reflections. These unwanted reflections, usually from stationary objects in the range bin of interest, tend to overwhelm signals from small displacements. In order to cancel these reflections, we recommend covering all flat surfaces in the direction of the beam with eccosorb, a mmW absorbing material.

We would have liked to have made our system mobile so that we could have changed the environments where we took our measurements. Making the system mobile would also allow us to take measurements over much larger ranges. In order to mobilize the system, we recommend moving the system onto a cart. In mobilizing the system, we also recommend replacing the 6 cm Teflon lenses with larger optics. These larger optics would allow for more targets to be placed in the path of the beam without completely blocking the beam while increasing the radiation received with a larger optic.

Through performing this experiment, we formulated an idea for a modified FMCW radar system that would allow for greater range resolution and more accurate displacement measurements. This system would employ adaptive waveform, machine learning, cognitive radio methods to continuously change the size of the range bins. Using this method, the system would theoretically be able to perfectly measure the displacement of many targets and optimize the measurement of the displacement of multiple targets in different range bins.

6 References

[1] M. I. Skolnik, "Radar," 28 December 2018. [Online]. Available: https://www.britannica.com/technology/radar/History-of-radar. [Accessed 21 April 2019].

[2] A. Dallinger, S. Schelkshorn and J. Detlefsen, "Broadband Millimeter-wave FMCW Radar for Imaging of Humans," IEEE, 2006.

[3] D. T. Petkie, E. Bryan, C. Benton and B. D. Rigling, "Millimeter-wave radar systems for biometric applications," *Millimetre Wave and Terahertz Sensors and Technology II,* vol. 7485, 2009.

[4] A. Marsh, "From World War II Radar to Microwave Popcorn, the Cavity Magnetron Was There," 31 October 2018. [Online]. Available: https://spectrum.ieee.org/tech-history/dawn-of-electronics/from-world-war-ii-radar-to-microwave-popcorn-the-cavity-magnetron-was-there. [Accessed 21 April 2019].

[5] C. Wolff, "Radar Tutorial," 1998. [Online]. Available: http://www.radartutorial.eu/02.basics/Pulse%20Radar.en.html. [Accessed 17 April 2019].

[6] J. Tu, T. Hwang and J. Lin, "Respiration Rate Measurement Under 1-D Body Motion Using Single Continuous-Wave Doppler Radar Vital Sign Detection System," *IEEE TRANSACTIONS ON MICROWAVE THEORY AND TECHNIQUES,* vol. 64, no. 6, pp. 1937-1948, 2016.

[7] G. M. Brooker, "Understanding Millimetre Wave FMCW Radars," University of Sydney, Sydney, 2005.

[8] D. M. Sheen, D. L. McMakin and T. E. Hall, "Three-Dimensional Millimeter-Wave Imaging for Concealed Weapon Detection," *IEEE TRANSACTIONS ON MICROWAVE THEORY AND TECHNIQUES,* vol. 49, no. 9, pp. 1581-1592, 2001.

[9] D. T. Petkie, E. Bryan, C. Benton, C. Phelps, J. Yoakum, M. Rogers and A. Reed, "Remote respiration and heart rate monitoring with millimeter-wave/terahertz radars," *Proceedings of SPIE,* vol. 7117, 2008.

[10] L3 Security & Detection Systems, "Advanced Personnel Screening," L3 Security & Detection Systems, 2019. [Online]. Available: https://www.sds.l3t.com/products/advancedimagingtech.htm. [Accessed 25 April 2019].

[11] R. Zhang and S. Cao, "3D Imaging Millimeter Wave Circular Synthetic Aperture Radar," *Sensors,* vol. 17, no. 1419, 2017.

[12] C. d. Looper, "Verizon 5G rollout: Here is everything you need to know," 4 April 2019. [Online]. Available: https://www.digitaltrends.com/mobile/verizon-5g-rollout/. [Accessed 21 April 2019].

[13] E. Schulze, "5G is barely here and some people, not just President Trump, are talking about 6G," 4 March 2019. [Online]. Available: 2019. [Accessed 21 April 2019].

[14] H. D. Young and R. A. Freedman, "35.5 The Michelson Interferometer," in *University Physics with Modern Physics*, New York, Pearson Education, 2016, pp. 1176-1178.

[15] L. Motta, "Michelson Interferometer," Wolfram Research, 2007. [Online]. Available: http://scienceworld.wolfram.com/physics/MichelsonInterferometer.html. [Accessed 21 April 2019].

[16] S. R. Systems, *About Lock-In Amplifiers,* Sunnyvale: Stanford Research Systems.

[17] M. C. Moulton, M. L. Bischoff, C. Benton and D. T. Petkie, "Micro-Doppler radar signatures of human activity," *SPIE Millimetre Wave and Terahertz Sensors and Technology III,* vol. 7837, 2010.

Appendix A: System Components

- Agilent E8254A, 250 kHz-40 GHz RF signal generator

- Virginia Diodes 80-120 GHz, 12 times frequency multiplier chain

- BK Precision, DC power supply (used to power the active frequency multiplier)

- Mylar 50/50 beam splitter

- Custom 2 inch Teflon lenses with 100 mm and 120 mm focal lengths

- Newmark Systems NLS4-12-16-1, 12-inch linear stage

- Newmark Systems NSC M4, Motor controller

- ELVA ZBD-08, 90-140 GHz detector

- Stanford Research SR560, Low-noise Preamplifier

- Stanford Research SR830, Lock-in amplifier

- Anfatec USB LockIn 250, Lock-in amplifier

- National Instruments BNC 2110 DAQ, Data acquisition card

- Keysight DSOX 1102G, 70MHz oscilloscope